

Methane formation in cold regions from carbon atoms and molecular hydrogen

THANJA LAMBERTS ^{1,2} GLEB FEDOSEEV ^{2,3} MARC VAN HEMERT,¹ DANNA QASIM ^{2,4} KO-JU CHUANG ² JULIA C. SANTOS ² AND HAROLD LINNARTZ ²

¹*Leiden Institute of Chemistry, Gorlaeus Laboratories, Leiden University, PO Box 9502, 2300 RA Leiden, The Netherlands*

²*Laboratory for Astrophysics, Leiden Observatory, Leiden University, PO Box 9513, 2300 RA Leiden, The Netherlands*

³*Research Laboratory for Astrochemistry, Ural Federal University, Kuibysheva St. 48, 620026 Ekaterinburg, Russia*

⁴*Current address: Astrochemistry Laboratory, NASA Goddard Space Flight Center, Greenbelt, MD 20771, USA*

(Received; Revised; Accepted)

Submitted to ApJ

ABSTRACT

Methane is typically thought to be formed in the solid state on the surface of cold interstellar icy grain mantles *via* the successive atomic hydrogenation of a carbon atom. In the current work we investigate the potential role of molecular hydrogen in the CH₄ reaction network. We make use of an ultra-high vacuum cryogenic setup combining an atomic carbon atom beam and both atomic and/or molecular beams of hydrogen and deuterium on a H₂O ice. These experiments lead to the formation of methane isotopologues detected *in situ* through reflection absorption infrared spectroscopy. Most notably, CH₄ is formed in an experiment combining C atoms with H₂ on amorphous solid water, albeit slower than in experiments with H atoms present. Furthermore, CH₂D₂ is detected in an experiment of C atoms with H₂ and D₂ on H₂O ice. CD₄, however, is only formed when D atoms are present in the experiment. These findings have been rationalized by means of computational chemical insights. This leads to the following conclusions: a) the reaction C + H₂ → CH₂ can take place, although not barrierless in the presence of water, b) the reaction CH + H₂ → CH₃ is barrierless, but has not yet been included in astrochemical models, c) the reactions CH₂ + H₂ → CH₃ + H and CH₃ + H₂ → CH₄ + H can take place only *via* a tunneling mechanism and d) molecular hydrogen possibly plays a more important role in the solid-state formation of methane than assumed so far.

Keywords: astrochemistry — ISM: molecules — molecular processes — methods: laboratory: solid state — techniques: spectroscopic

1. INTRODUCTION

Methane, the smallest hydrocarbon, is one of the few molecules that have been detected in the solid phase in various regions in the interstellar medium (ISM) (Boogert et al. 2015). In fact, the first detection was a simultaneous gas phase and tentative solid phase identification, based on the ν_4 feature at 7.6 μm (Lacy et al. 1991) and meanwhile several in-depth observational studies have been reported (Boogert et al. 1996; Öberg et al. 2008). Early reports based on comparison to laboratory data indicated that methane likely resides in ice comprising polar component(s) (Boogert et al. 1996) and it was later postulated that H₂O is the primary candidate for this based on correlations between CH₄ and H₂O column densities (Öberg et al. 2008). This points to the fact that solid CH₄ is formed during the translucent phase of the evolutionary track of molecular clouds.

The solid-state formation of methane is typically assumed to follow four sequential atomic hydrogenation steps of the carbon atom in the ³P ground state ever since this was postulated in the late 1940s (van de Hulst 1946, 1949; D’Hendecourt et al. 1985; Brown et al. 1988; Brown & Charnley 1991). Recently, this route has been confirmed experimentally (Qasim et al. 2020) through

the simultaneous use of well-characterized C- and H-atom beams, following up on early work by (Hiraoka et al. 1998):

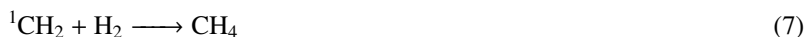


The hydrogen atom number density in molecular clouds is estimated to be around a few atoms/cm³, which is two to four orders of magnitude lower than the molecular hydrogen abundance depending on whether a translucent or dense cloud is concerned (van Dishoeck & Black 1988; Goldsmith & Li 2005). Therefore, also solid-state reactions with molecular hydrogen can be of great importance even when the corresponding rate constants are lower, as pointed out already in 1993 by Hasegawa & Herbst. For instance for the sequential hydrogenation of the O atom to eventually form water (Hiraoka et al. 1998; Ioppolo et al. 2008; Miyauchi et al. 2008) it has been shown that the reaction $\text{H}_2 + \text{OH} \longrightarrow \text{H}_2\text{O} + \text{H}$ can become more relevant than $\text{H} + \text{OH} \longrightarrow \text{H}_2\text{O}$ even though a considerable barrier is invoked (Cuppen & Herbst 2007; Furuya et al. 2015). Another example is the hydrogenation of carbon monoxide by UV-irradiation of mixed CO:H₂ ices Chuang et al. (2018). Despite such active involvement of H₂ in solid-state reactions, the molecular hydrogen abundances on ice surfaces in astrochemical microscopic models are often artificially reduced to save (a lot of) computational cost, *e.g.*, by decreasing the sticking coefficient (Lamberts et al. 2013; Vasyunin & Herbst 2013; Garrod 2013). We also want to point out that despite the fact that neutral carbon atoms are often thought to only be (abundantly) present in translucent regions (van Dishoeck & Black 1988; Snow & McCall 2006), there exists substantial literature that leads to believe that C[II] is more extended, possibly even into denser regions (Langer 1976; Keene et al. 1985; Papadopoulos et al. 2004; Burton et al. 2015; Bisbas et al. 2019).

For these reasons, we consider a number of reactions with molecular hydrogen in the context of methane formation. Firstly, the direct addition or insertion reactions:



Reaction 5, the first step in the reaction network, has been covered in a series of papers indicating that the reaction may readily take place in helium droplets (Krasnokutski et al. 2016; Henning & Krasnokutski 2019) and including this reaction in astrochemical models without a barrier was suggested recently (Simončič et al. 2020). The reaction



intuitively the most likely step to form methane, can only take place if methylene is in the excited singlet state, ¹CH₂ (Murrell et al. 1973; Bauschlicher et al. 1977). In the system currently under study, only ground-state ³CH₂ is expected to be present and therefore reaction 7 will not be further considered.

In terms of the chemical reaction network, there is furthermore the possibility of hydrogen abstraction, either from H₂ or from a CH_{*n*} fragment:



Reactions 8-11 are listed in the exothermic direction, and the reverse endothermic reactions are not expected to be important given the low temperatures involved ($\sim 10 - 20$ K). We assume that the exothermicities of the reactions are not significantly altered by the solid-state surroundings of the reaction site. This essentially translates into assuming that the binding energies of the reactants and products are similar. We also assume that the H atoms formed in reactions 10 and 11 immediately desorb, based on the argument of conservation of energy and momentum (Koning et al. 2013).

In the current manuscript, we revisit reaction 5 in water ices and extend the discussion on H₂ reactivity investigating the influence of reactions 6–11. We show that reactions 5, 6, 10, and 11 together can lead to the formation of methane, without the involvement of H-atoms. To achieve this, we make use of in-situ infrared spectroscopy to probe which methane isotopologues

Table 1. Summary of all performed experiments, organized along four selected sets. MDL, SUKO and MWAS refer to the used atomic and molecular deposition lines (see text). Furthermore the substrate temperature, the atomic and molecular fluxes and the total time of the experiment, from which the fluence can be derived, are listed. All fluxes give the effective value. Please note that H (H₂) and D (D₂) have different thermal velocities and sticking coefficients, thus a direct comparison should be done with care. Values in bold font underline the different settings within one series of measurements.

#	T K	H ₂ O cm ⁻² s ⁻¹	C cm ⁻² s ⁻¹	H cm ⁻² s ⁻¹	H ₂ cm ⁻² s ⁻¹	D cm ⁻² s ⁻¹	D ₂ cm ⁻² s ⁻¹	C:H:H ₂ :D:D ₂	Time (min)
		MDL	SUKO	MWAS			MDL		
1 A	10	8 × 10 ¹²	5 × 10 ¹¹	2 × 10 ¹²	1 × 10 ¹⁴			1:4:200:-:-	30
1 B	10	8 × 10 ¹²	5 × 10 ¹¹	2 × 10 ¹²	1 × 10 ¹⁴		1 × 10¹³	1:4:200:-:-20	30
1 C	10	8 × 10 ¹²	5 × 10 ¹¹	2 × 10 ¹²	1 × 10 ¹⁴		4 × 10¹³	1:4:200:-:-80	30
		MDL	SUKO	MDL		MWAS			
2 A	10	8 × 10 ¹²	5 × 10 ¹¹			1.5 × 10 ¹²	6 × 10 ¹³	1:-:-:3:120	30
2 B	10	8 × 10 ¹²	5 × 10 ¹¹		5 × 10¹³	1.5 × 10 ¹²	6 × 10 ¹³	1:-:100:3:120	30
2 C	10	8 × 10 ¹²	5 × 10 ¹¹		2 × 10¹⁴	1.5 × 10 ¹²	6 × 10 ¹³	1:-:400:3:120	60
		MDL	SUKO	MDL		MDL			
3 A	10	1.2 × 10 ¹³	5 × 10 ¹¹				1 × 10¹⁴	1:-:-:-:200	60
3 B	10	1.2 × 10 ¹³	5 × 10 ¹¹		1 × 10¹⁴		1 × 10¹⁴	1:-:200:-:-:200	240
#	T K	D ₂ O cm ⁻² s ⁻¹	C cm ⁻² s ⁻¹	H cm ⁻² s ⁻¹	H ₂ cm ⁻² s ⁻¹	D cm ⁻² s ⁻¹	D ₂ cm ⁻² s ⁻¹		Time (min)
		MDL	SUKO	MDL					
4 A	10	1.4 × 10 ¹³	5 × 10 ¹¹		2.5 × 10 ¹⁴			1:-:500:-:-	60
4 B	25	1.4 × 10 ¹³	5 × 10 ¹¹		2.5 × 10 ¹⁴			1:-:500:-:-	60

are formed via reaction of ³C with selected combinations of atomic and molecular hydrogen (H, H₂) and deuterium (D, D₂) on representative interstellar water-rich ice analogs.

This manuscript is organized in the following way. The experimental details and results are discussed in sections 2.1 and 3. Furthermore, we position the chemical network listed above within the context of the extensive theoretical chemical literature, complemented by additional computations presented that explicitly take into account the role of the water ice surface. This helps to disentangle which reactions are likely to take place throughout the various experiments, as outlined in Section 2.2 and discussed in section 4. Solid methane is hard to observe from ground-based observatories because of telluric pollution. Observations from space offer an alternative. Solid methane has been observed already with the Spitzer space telescope (Öberg et al. 2008). Because of its higher sensitivity and spatial resolution, the James Webb Space Telescope (JWST) is expected to substantially extend on these observations. The present experimental work and theoretical approach fits worldwide efforts to prepare for upcoming JWST observations. In section 5 the astrochemical implications and conclusions of this work are presented.

2. METHODOLOGY

2.1. Experimental methodology

The experimental setup used is SURFRESIDE³, an ultra-high vacuum system with three atomic beam lines (Ioppolo et al. 2013; Qasim et al. 2020). For the purpose of our study, only H/D and C atom beam lines are used. Ices are grown on a gold-coated copper substrate that is attached to the cold finger of a closed-cycle He cryostat in the centre of the main UHV chamber with a base pressure on the order of 10⁻¹⁰ mbar. Co-deposition experiments of H₂O + ³C and combinations of H, D, H₂, and/or D₂ are performed that lead to the growth of a mixed ice at 10 K. Mixed H/H₂- or D/D₂-beams are obtained by (partial) dissociation of molecular H₂ (Linde 5.0) or D₂ (Linde 2.8) in a microwave discharge source (MWAS, Oxford Scientific, (Schmidt et al. 1996; Anton et al. 2000)) in a separate vacuum chamber with a base pressure of ~10⁻⁹ mbar. Note that charged particles are removed by means of applying an electric field that deflects these species. Excited-state species are de-excited through collisions with the walls of a U-shaped quartz pipe at room temperature placed along the beam path prior to the molecules entering the main chamber. A customized SUKO-A 40 C-atom source (Qasim et al. 2020) based on a commercial design (Dr. Eberl, MBE, (Krasnokutski & Huysen 2014; Albar et al. 2017)) produces a beam of carbon atoms in the ³P ground state with a C_n/C (n>1) ratio of less than 0.01. This source is located in another separate vacuum chamber with a base pressure (3-5)×10⁻⁹ mbar. A

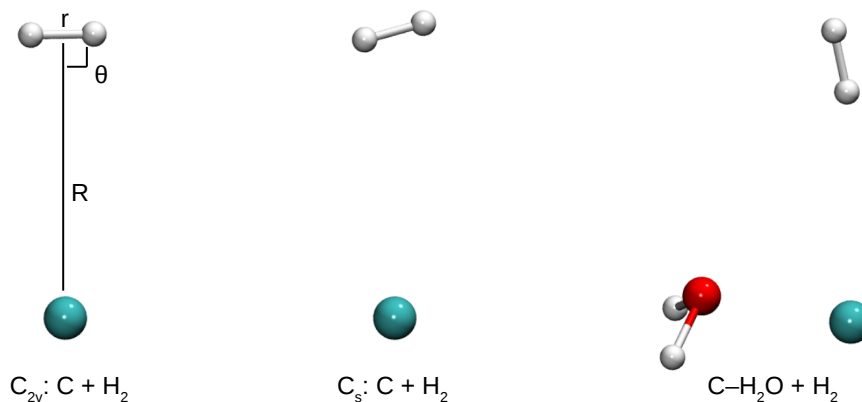


Figure 1. Three cases studied for the reaction $C + H_2 \longrightarrow CH_2$.

series of apertures is used to collimate the C-atom beam on the substrate avoiding deposition of carbon on the walls of the main UHV chamber. Note that CO and CO₂ are known (minor) contaminants in the C-atom beam. A third vacuum chamber with a base pressure of $\sim 10^{-9}$ mbar is used to generate a molecular H₂O (Milli-Q) or D₂O (Sigma-Aldrich 99.9 atom% D) beam for simultaneous deposition (MDL). We use an overabundance of H₂O, to mimic a polar ice environment, *e.g.*, in agreement with the previously mentioned correlation between observed CH₄ and H₂O column densities. The atomic and molecular fluxes are listed in Table 1, in which all experiments are summarized. The uncertainty in the flux determination is roughly a factor two. The initial reactants and formed products are monitored via Reflection Absorption InfraRed Spectroscopy (RAIRS, (Greenler 1966)) in the solid state *in situ*. These experiments are organized along four different series in which relevant parameters are systematically varied.

2.2. Computational methodology

The primary focus of our own calculations is on the reaction $C + H_2 \longrightarrow CH_2$, since it is the first and most determining step in the reaction network mentioned above leading to CH₄. Moreover, the carbon atom is known to be highly reactive (Kim et al. 2003). However, despite the work by Simončič et al. (2020), to date it has not been looked at in detail for surface chemistry purposes. Note that for the other possible steps (reactions 6–11), we draw from previous studies available from the literature.

We take a threefold approach, see also Fig. 1, to understand the reactivity of $C + H_2 \longrightarrow CH_2$:

1. a gas-phase calculation of a highly symmetric orientation of C with respect to H₂ (C_{2v} symmetry) - meant to compare against previous results,
2. a gas-phase calculation of a low symmetry orientation of C with respect to H₂ (C_s symmetry) - meant to be a first step towards a realistic symmetry-broken orientation on a surface,
3. a calculation of the reaction of H₂ with a C atom bound to a single H₂O molecule (no symmetry) - meant as a first step towards understanding the reaction with a bound carbon atom on a water ice.

When an H₂ molecule approaches a carbon atom in its ³P ground state the encounter can occur on three, initially degenerate, potential surfaces (PESs). Important to take into account is the alignment of the two singly occupied 2p orbitals of the carbon atom. When the orientation of the H₂ molecule is perpendicular to the direction of approach, there is a C_{2v} symmetry and the three surfaces are ³B₁, ³B₂ and ³A₂. For all three surfaces the energy was calculated as a function of the Jacobi coordinates R as the distance between C and the center-of-mass of H₂, r as the H–H distance, and $\theta = 90^\circ$ as the angle between R and r , see again Fig. 1. All calculations were repeated in C_s symmetry where the angle θ was reduced to 80° , while keeping the CAS/CI parameters as closely as possible to the ones used in the C_{2v} case. In C_s symmetry two ³A'' states are relevant. Subsequently, to find possible reaction paths, the location of the crossing (seam) between the ³B₁ and ³A₂ for C_{2v} and the two ³A'' surfaces for C_s was searched for by scanning these surfaces with small steps in the $R \approx r \approx 1$ Å range. These calculations have been performed using Molpro (Werner et al. 2012, 2018) with the AVQZ basis set (Woon & Dunning 1993; Dunning et al. 2001). The CASSCF calculation had 8 electrons in 8 orbitals, while state averaging over singlet and triplet states, each with 4 lowest roots, both for C_{2v} and C_s symmetries.

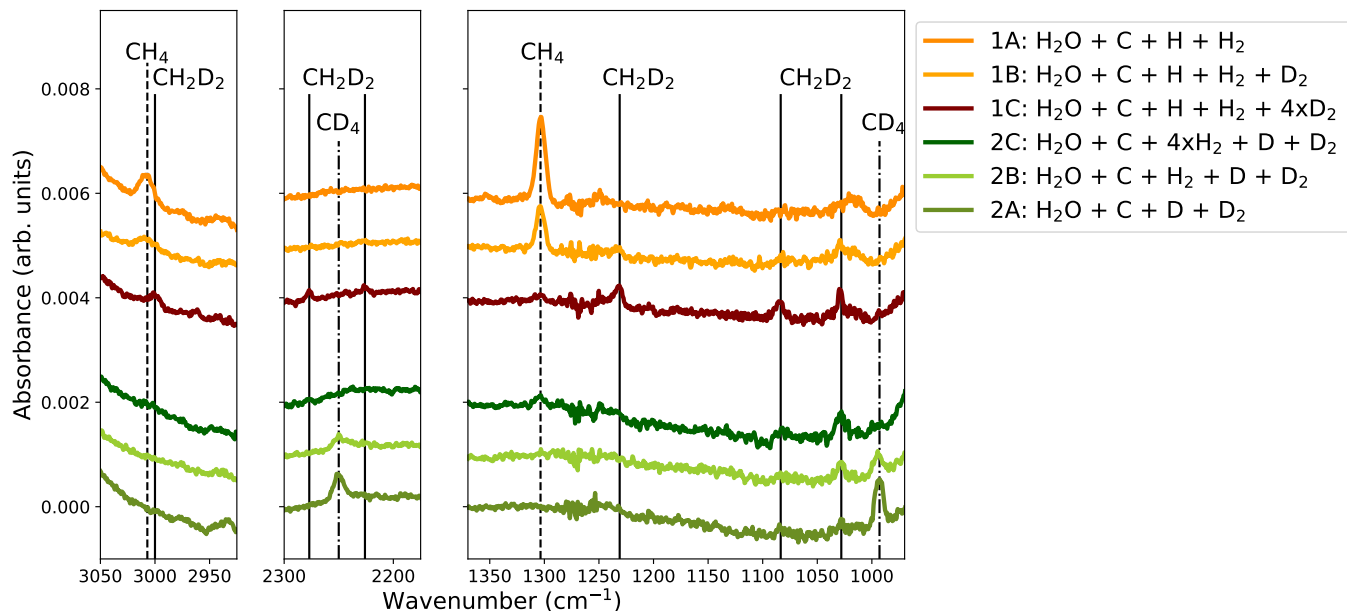


Figure 2. RAIR spectra of experimental series 1 and 2, the exact experimental conditions can be found in Table 1. The dashed vertical lines indicate the peak positions of CH₄, the solid vertical lines indicate CH₂D₂, the dash-dotted lines indicate D₂CO, see Table 4 in the appendix for specific peak positions.

In order to test – for the first time – the influence of the strong adsorption of the carbon atom atop water ice on the reactivity of the carbon atom with H₂ we have performed a nudged elastic band (NEB) calculation for the reaction of H₂ with a carbon atom bound to a water molecule, *i.e.*, C–H₂O complex. This was followed by a transition state optimization applying the dimer method with the B3LYP functional (Becke 1988, 1993; Lee et al. 1988) and using DL-find in Chemshell (Kästner et al. 2009; Metz et al. 2014). For the resulting reactant, transition, and product states, single-point energies were calculated with both MRCI/AVTZ (Werner & Knowles 1988; Dunning 1989; Kendall et al. 1992) and CCSD(T)-F12a/VTZ-F12 (Adler et al. 2007; Knizia et al. 2009; Peterson et al. 2008) in Molpro version 2020 (Werner et al. 2020). All geometries were re-optimized at the CCSD(T)-F12a/VTZ-F12 level of theory in Molpro. MRCI calculations are, in principle, warranted for systems where multi-reference effects can be expected, such as here where a triplet ground state carbon atom is involved. We do note, however, that the *T*1 and *D*1 values in both CCSD(T)-F12 calculations are (well) below the common threshold values of *T*1 < 0.04 and *D*1 < 0.05 (Janssen & Nielsen 1998; Lambert et al. 2006). Indeed, the MRCI single-point energy calculations indicate that the main contribution of a Slater determinant to the wave function has reference coefficients of about 0.93-0.94 for all C – H₂O – H₂ geometries.

3. EXPERIMENTAL RESULTS

Figure 2 shows the RAIR spectra of experimental series 1 and 2, over the wavenumber ranges that include all relevant spectroscopic bands of CH₄, CD₄, and CH₂D₂, indicated by the vertical lines in the figure. Other detected species are listed in Table 4 in Appendix B.

Experiments 1A and 2A (NB: top and bottom graph in Fig. 2) serve as a control experiment and can be directly compared to previous work (Qasim et al. 2020): indeed the formation of CH₄ and CD₄ is clearly confirmed by the presence of both the ν_3 and ν_4 vibrational modes. Molecular deuterium (hydrogen) is introduced in experiment 1B (2B) and increased in experiment 1C (2C) and a concomitant decrease of CH₄ (CD₄) can be easily observed. At the same time, several CH₂D₂ absorption features appear in these four experiments, the most intense peak at 1028 cm⁻¹. Experiment 1C shows the most apparent, multi-line detection of doubly deuterated methane as a result of the advantageous ratio between all reactants, *i.e.*, C:H:H₂:D₂ = 1:4:200:80, see also Table 1.

Because doubly deuterated methane is observed in experiments for which either hydrogen or deuterium is present only in the molecular form, at least one reaction with a molecular species must take place throughout the course of methane formation. This is further supported by a tentative CH₄ detection at 1303 cm⁻¹ in experiment 2C, *i.e.*, in an experiment with hydrogen present only in the molecular form.

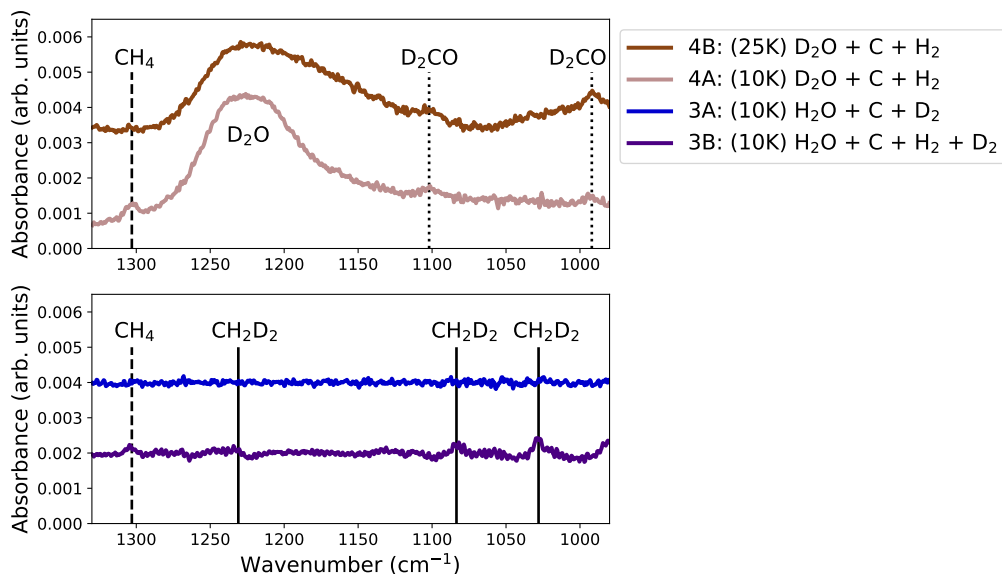


Figure 3. RAIR spectra of experiments 1C, 2C, 3A, 3B, 4A, and 4B, the exact experimental conditions can be found in Table 1. The dashed vertical lines indicate the peak position of CH₄, the solid vertical lines indicate CH₂D₂, the dotted lines indicate D₂CO, and the broad peak is caused by D₂O indicated directly in the plot, see Table 4 in the appendix for specific peak positions.

This tentative detection was the reason to perform experimental series 3 and 4 to further investigate whether methane indeed can be formed without the presence of atomic species. In order to increase the signal-to-noise ratio, these experiments have been run over longer times, as indicated in Table 1. These experiments clearly result in a lower overall formation rate of methane in comparison to interactions with atomic species. The resulting thick ices (~ 200 ML) and concomitant interference patterns over the full range of the IR spectra have led to presenting baseline-corrected spectra of the region of interest only ($1330 - 980$ cm⁻¹) depicted in Fig. 3. The baseline-correction includes the subtraction of known components of the purging gas used along the path of the infrared beam, *i.e.*, outside the vacuum chamber. Experiment 3B, consisting of C + H₂ + D₂ on H₂O ice, shows a clear detection of the two main CH₂D₂ peaks at 1083 and 1028 cm⁻¹. In other words, CH₂D₂ has been formed from carbon atoms and molecular species only. However, the yield of CH₂D₂ is significantly less than in experiments 1C and 2C. Experiments 3A and 4A represent a co-deposition of C + D₂ + H₂O, and C + H₂ + D₂O, respectively. In experiment 3A no CD₄ is detected, while experiment 4A shows a clear solid-state CH₄ detection. In other words in the reaction network for the formation of methane from carbon atoms and molecular hydrogen there is an isotope effect present, which hints for the importance of tunneling in one, or more, of the involved reactions.

Experiment 4B, another control experiment, performed at 25 K, *i.e.*, above the desorption temperature of atomic or molecular hydrogen, shows no CH₄ formation in the solid state confirming that the processes we are studying take place at the surface at low temperatures.

Finally, no CD₃H or CH₃D was detected in any of the experiments which can be attributed to a combination of isotope effects, lower band strengths, and competition between tunneling and barrierless reactions in the network. A full rationale for the lack of these signals is given in Appendix A.

We can summarize the experimental findings as follows:

1. CH₄ is detected in experiments on a water ice using both H atoms and H₂ molecules as well as in experiments using only H₂, albeit with a lower efficiency,
2. CD₄ is detected only in experiments where D atoms are present,
3. CH₂D₂ can be detected in experiments that use simultaneously both atomic and molecular hydrogen or deuterium sources,
4. CH₂D₂ can also be detected in experiments that use exclusively molecular H₂ and D₂,
5. Neither CH₃D nor CHD₃ are detected,
6. All studied reactions take place on the cold ice surface.

4. THEORETICAL RESULTS

Table 2. Activation and reaction energies in kJ/mol, E_{act} and E_{react} respectively, for the reaction of the C–H₂O complex with H₂ leading to the CH₂–H₂O complex. The interaction energy, E_{int} of the CH₂–H₂O complex is also given.

	B3LYP	MRCI / B3LYP	CCSD(T)-F12 / B3LYP	CCSD(T)-F12
$E_{\text{int, C-H}_2\text{O}}$	-52.9			-36.1
$E_{\text{act, C-H}_2\text{O} + \text{H}_2}$	30.4	30.0	27.3	30.4
$E_{\text{react, C-H}_2\text{O} + \text{H}_2}$	-294.3	-281.5	-303.1	-300.5
$E_{\text{int, CH}_2\text{-H}_2\text{O}}$	-8.0			-7.1

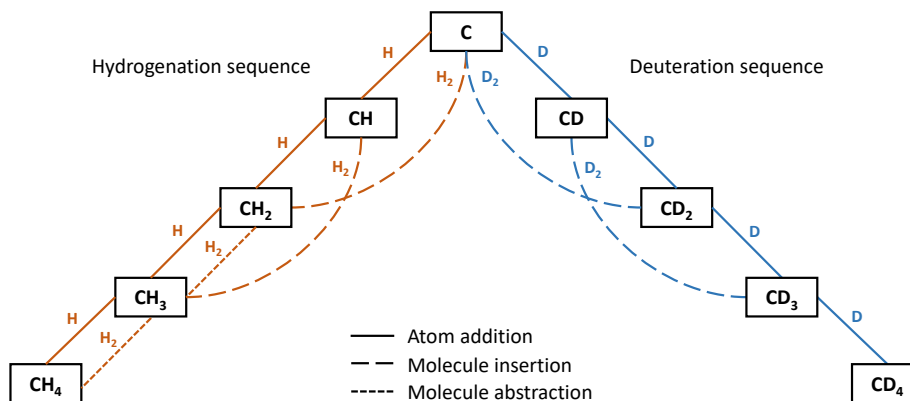


Figure 4. Three types of reactions are considered to lead to the formation of CH₄ or CD₄: H or D addition (Qasim et al. 2020), H₂ or D₂ insertion (Krasnokutski et al. (2016); Simončič et al. (2020) and this work), and H₂ abstraction (this work). We assume that the latter is not efficient with D₂, based on the involved high barrier and lack of tunneling efficiency.

This section focuses on explaining the experimental results by looking in detail at theoretical chemical studies of reactions 5–11. Reactions 1–4 have been extensively discussed in Qasim et al. (2020) and will therefore not be further dealt with here. A summary of all relevant reaction steps can be found in Fig. 4

Section 4.1 contains predominantly results from our own calculations, while sections 4.2 and 4.3 are based on previous results available from the literature.

4.1. Reactions on the CH₂ PES

All three calculated C_{2v} surfaces for the C + H₂ reaction, ³B₁, ³B₂ and ³A₂ are degenerate for large R (C–H₂ distance) with an energy of ~330 kJ/mol above the ³B₁ CH₂ ground state, see also Fig. 6 in Appendix C. We find a crossing between the ³A₂ and ³B₁ surfaces at $R = 1.05$ Å and $r = 1.17$ Å at an energy equal to the asymptotic value of C + H₂. In agreement with Gamallo et al. (2012), under the assumption that a transition from the ³A₂ to the ³B₁ occurs via a conical intersection, there is no barrier. When the symmetry is lowered to C_s, which should more closely resemble the situation on an ice surface, by giving up the perpendicular orientation and instead choosing $\theta = 80^\circ$, both the ³B₁ and ³A₂ surfaces become of the same ³A'' symmetry and a reaction can take place without a serious energetic barrier. A small hump can be found along the path at $R = 1.08$ Å and $r = 1$ Å, but this remains below the C + H₂ asymptotic value, see Fig. 6.

While the notion of the reaction C + H₂ → CH₂ being barrierless seems in line with recent literature (Gamallo et al. 2012; Simončič et al. 2020), two important things have up to now not been explicitly taken into account. First of all, at the (avoided) crossing of the C_{2v} potential energy surfaces, there is a change in electron configuration. The dominant contribution to the wavefunction on the ³A₂ surface consists out of an occupation for the 6 valence electrons of (2a₁)² (3a₁)² (1b₁)¹ (1b₂)¹ and this needs to change to (2a₁)² (3a₁)¹ (1b₁)¹ (1b₂)² before reaching the ³B₁ CH₂ ground state. This means an electron has to move from a pz orbital on the carbon atom into a py orbital, which can impede the reaction from taking place, even if energetically there is no barrier. This argument still holds in the case of the low-symmetry C_s surface where the electron configuration also changes upon decreasing R and increasing r , i.e., reacting towards CH₂.

Secondly, the known strong interaction of ^3P carbon atom with a H_2O molecule or cluster (Wakelam et al. 2017; Shimonishi et al. 2018; Duflo et al. 2021; Molpeceres et al. 2021) might drastically change the energetics of the reaction. Estimates on the exact interaction energy depend on the number of water molecules considered and vary between ~ 35 and ~ 115 kJ/mol, much larger than a typical water hydrogen bond of some ~ 22 kJ/mol. Table 2 gives an overview of the interaction energy of the $\text{C}-\text{H}_2\text{O}$ complex and the activation and reaction energy of the reaction $\text{H}_2 + \text{C} - \text{H}_2\text{O} \longrightarrow \text{CH}_2 - \text{H}_2\text{O}$ for different levels of theory. A sizable barrier of 27-30 kJ/mol is found, which certainly cannot be trivially overcome at 10 K. This demonstrates that while the $\text{C} + \text{H}_2$ reaction proceeds barrierlessly in helium droplets (Krasnokutski et al. 2016; Henning & Krasnokutski 2019) this is unlikely to be the case on water surfaces. Because this is a proof-of-principle calculation, and more extensive work should be done on $\text{C}-(\text{H}_2\text{O})_n$ clusters with $n > 1$, we cannot elaborate on the expected isotope effect of this reaction, but we assume that this reaction on a water ice proceeds with an (effective) barrier and will thus be slower with D_2 compared to H_2 .

Reaction 8, $\text{CH} + \text{H} \longrightarrow ^3\text{C} + \text{H}_2$, has to proceed through a CH_2 intermediate, as can be seen in Fig. 2 of Gamallo et al. (2012). While this is a realistic scenario in gas-phase experiments in the low-pressure regime where intermediates can convert the reaction energy as internal energy to overcome subsequent barriers, such intermediates are expected to be quenched on a surface by rapid (< 1 ps) energy dissipation to a water ice Fredon et al. (2021). Therefore, reaction 8 turns effectively into reaction 5 on a surface.

4.2. Reactions on the CH_3 PES

The exchange reaction $\text{CH} + \text{H}_2 \rightleftharpoons \text{CH}_2 + \text{H}$ has been previously studied in the gas phase (McIlroy & Tully 1993; Medvedev et al. 2006; González et al. 2011). In particular, Medvedev et al. (2006) showed that the reaction proceeds through an activated CH_3^* intermediate, which is formed *via* a barrierless pathway in both the forward and backward direction of the reaction, *i.e.*, $\text{CH} + \text{H}_2 \rightleftharpoons \text{CH}_3^* \rightleftharpoons \text{CH}_2 + \text{H}$. In the low-pressure regime, González et al. (2011) showed that the three hydrogen atoms become equivalent, as a result of the long-lived CH_3^* complex. In the high-pressure regime, on the other hand, McIlroy & Tully (1993) indicated that collisional stabilization to form ground-state CH_3 dominates. A reaction taking place on an ice surface can be seen as an extreme case of the high-pressure limit, in which the ice acts as a third body to take up the excess energy of the reaction (see above). Given the barrierless nature of the PES, we expect no isotope effect here. In other words, it is highly likely that reaction 6 will lead barrierlessly to the formation of CH_3 on the ice, while reaction 9 is unlikely to take place at all and will revert simply to reaction 3, also forming CH_3 . This serves as an explanation why CH_2D_2 is detected in experimental sets 1 and 2, since the barrierless nature leads to a lack of isotope effect.

4.3. Hydrogen abstraction reactions

The two remaining reactions with molecular hydrogen, reactions 10 and 11, have been previously studied, see the reported barriers in Table 3. Both reactions can only take place when a considerable barrier (> 44 kJ/mol) is overcome, for which tunneling needs to be invoked to reach rate constants that are high enough for the reaction to be able to take place at the low temperatures in dense molecular clouds. The effect of tunneling can be accurately included by means of instanton theory (Langer 1976; Miller 1975; Callan & Coleman 1977; Rommel & Kästner 2011; Richardson 2016). Although Beyer et al. (2016) indeed calculated instanton rate constants for the reaction $\text{CH}_3 + \text{H}_2$, they provided only bimolecular rate constants, whereas unimolecular rate constants are those relevant for Langmuir-Hinshelwood type surface reactions (Lamberts et al. 2016; Meisner et al. 2017). Given the high activation barriers, about double as for the reaction $\text{H}_2 + \text{OH} \longrightarrow \text{H}_2\text{O} + \text{H}$ (Meisner et al. 2017) and slightly above that of $\text{H} + \text{H}_2\text{O}_2 \longrightarrow \text{H}_2 + \text{HO}_2$ (Lamberts et al. 2016), relatively low rate constants are expected. While the quantitative calculations will be the topic of a future study, these two reactions are expected to show significant isotope effects and this explains also without further theory why the experiments with only D_2 as a source of deuterium do not lead to a CD_4 detection.

5. ASTROCHEMICAL IMPLICATIONS AND CONCLUSIONS

Currently, the main formation pathway of methane is thought to be through the reactions 1-4. Reactions 5, 10, and 11 are included in some astrochemical models, however, in most studies the initial guesses by (Hasegawa & Herbst 1993) are used, see for instance the current surface reactions in the KIDA database (Wakelam et al. 2015). Reaction 6, $\text{CH} + \text{H}_2 \longrightarrow \text{CH}_3$, is usually not included at all. For the interpretation of astronomical data, specifically those obtained by JWST in the nearby future, it is important for models to take into account that:

1. The reaction $\text{C} + \text{H}_2 \longrightarrow \text{CH}_2$ is unlikely to proceed *via* a fully barrierless mechanism on water ices and an isotope effect is yet to be determined.
2. The reaction $\text{CH} + \text{H}_2 \longrightarrow \text{CH}_3$ on the other hand is expected to take place readily and barrierlessly without an isotope effect.

Table 3. Activation energies from predominantly theoretical chemical literature for the reactions 1–11 in kJ/mol.

Reaction	ΔE_{act}	Ref.
(1) ${}^3\text{C} + \text{H} \longrightarrow \text{CH}$	0	[1]
(2) $\text{CH} + \text{H} \longrightarrow \text{CH}_2$	0	[2]
(3) ${}^3\text{CH}_2 + \text{H} \longrightarrow \text{CH}_3$	0	[3]
(4) $\text{CH}_3 + \text{H} \longrightarrow \text{CH}_4$	0	[4]
(5) ${}^3\text{C} + \text{H}_2 \longrightarrow {}^3\text{CH}_2$	27 – 30 ^a	[2]
(6) $\text{CH} + \text{H}_2 \longrightarrow \text{CH}_3$	0	[3]
(8) $\text{CH} + \text{H} \longrightarrow {}^3\text{C} + \text{H}_2$	– ^b	[2]
(9) $\text{CH}_2 + \text{H} \longrightarrow \text{CH} + \text{H}_2$	– ^c	[3]
(10) ${}^3\text{CH}_2 + \text{H}_2 \longrightarrow \text{CH}_3 + \text{H}$	49	[5]
(11) $\text{CH}_3 + \text{H}_2 \longrightarrow \text{CH}_4 + \text{H}$	44	[6]

^a Cannot be trivially determined due to conical intersection and strong C–H₂O interaction, see Section 4.1

^b The reaction is likely quenched in the CH₂ ground state, see Section 4.1 and (Gamallo et al. 2012), effectively changing the reaction to 2

^c Reaction is determined by the relaxation of the CH₃* intermediate see Section 4.2, and thus leads to reaction 3

References—[1] Qasim et al. (2020); [2] Harding et al. (1993); van Harreveld et al. (2002); Gamallo et al. (2012); this work; [3] McIlroy & Tully (1993); Medvedev et al. (2006); González et al. (2011); [4] Duchovic & Hase (1985); [5] Baskin et al. (1974); Bauschlicher (1978); [6] Li et al. (2015); Beyer et al. (2016)

3. The abstraction reactions $\text{CH}_2 + \text{H}_2 \longrightarrow \text{CH}_3 + \text{H}$ and $\text{CH}_3 + \text{H}_2 \longrightarrow \text{CH}_4 + \text{H}$ are expected to take place *via* a tunneling mechanism and a pronounced isotope effect is expected.

The points above are summarized in Table 3 and Fig. 4.

The main finding is that H₂ plays a role in the solid state formation of interstellar methane. CH₄ can be efficiently formed without invoking any H-atoms at all in our experiments, which is supported by our own calculations as well as theoretical results found in physical chemical literature. Thus, under physical conditions where H₂ is much more abundant than H atoms and taking into account that H₂ sticks to the surface at higher temperatures than H, methane formation from C atoms and H₂ (and HD, D₂) molecules is a reaction route that should be taken into account. In the end, both H₂ and H abundances as well as their respective reaction efficiencies with carbon atoms determine the relative impact of both mechanisms, for which dedicated modeling will be needed. The finding that a C + H₂ route also leads to methane formation has the following implications:

1. The formation of CH₄ can take place at ‘higher’ temperatures, *e.g.*, 20 K instead of 10 K, because of the stronger binding of H₂ molecules to the ice surface,
2. CH₄ can be formed in the ice bulk through the interaction of entrapped H₂ with CH_{*n*} radicals obtained by dissociation of hydrocarbons from UV-photons or cosmic ray particles,
3. Deuterium fractionation of methane is not only dictated by D/H ratios but also by (a) the respective abundances of D₂ and HD with respect to H₂ on the surface and (b) an isotope effect is expected because of the presence or lack of a barrier, see for instance Fig. 5,
4. While Qasim et al. (2020) focused on confirming the atomic hydrogenation route of carbon to form CH₄, here we show that not only reactions with H, but also H₂ chemistry overall should be fully incorporated into astrochemical models. This is particularly true for models that include microscopic detail, despite the increase in computational cost.

Software: Matplotlib (Hunter 2007), Numpy (van der Walt et al. 2011), Jupyter (Kluyver et al. 2016), Chemshell (Metz et al. 2014), Molpro (Werner et al. 2012)

ACKNOWLEDGMENTS

T.L. is grateful for support from NWO via a VENI fellowship (722.017.008). G.F. acknowledges financial support from the Russian Ministry of Science and Higher Education via the State Assignment Contract FEUZ-2020-0038. This research benefited from the financial support from the Dutch Astrochemistry Network II (DANII). Further support includes a VICI grant of NWO (the Netherlands Organization for Scientific Research). Funding by NOVA (the Netherlands Research School for Astronomy) is acknowledged.

APPENDIX

A. REACTION ROUTES FOR THE FORMATION OF METHANE ISOTOPOLOGUES

Below we explain the reaction pathways that lead to the formation of methane isotopologues of the form $\text{CH}_n\text{D}_{4-n}$ with $n = 0 - 4$ in the experimental series 1 – 4. Please note that the reactions considered barrierless are reactions 1–4 and 6 and these are expected to take place without an isotope effect. Reaction 5 is likely possible both with H_2 and D_2 , although it is currently unclear whether the rate constant is determined by the change needed in electron configuration and/or a barrier on a water-rich surface. It is possible that the reaction is slower with D_2 . Reactions 10 and 11 can only take place via tunneling and, given the high barrier, these reactions are expected to be very slow with D_2 . In Fig. 5 three networks are depicted, analogously to Fig. 4, one for each deuteration experiment. As in Fig. 4, three types of reactions are considered, H/D atom addition, H_2/D_2 insertion, and H_2 abstraction reactions. Note that we deliberately choose not to include D_2 abstraction reactions, because of the high barrier. Finally, we assume that the H or D atoms formed *in situ* do not take part in subsequent reactions, but desorb instead. We base this on the argument of conservation of energy and momentum (Koning et al. 2013).

The experiments are discussed below in order of increasing complexity.

A.1. Experiments 3 and 4: $\text{C} + \text{H}_2$ and/or D_2

The experiment (4A) with $\text{C} + \text{H}_2$ leads clearly to the formation of CH_4 , while an experiment (3A) with $\text{C} + \text{D}_2$ does not lead to a CD_4 detection. At the same time experiment 3B with $\text{C} + \text{H}_2 + \text{D}_2$ shows the formation of CH_2D_2 and CH_4 , but not CD_4 . This can be understood by considering the reactions presented in the top panel of Fig. 5.

A.2. Experiment 1: $\text{C} + \text{H} + \text{H}_2 + \text{D}_2$

Throughout the series for experiment 1 the only methane isotopologue species observed are CH_4 and CH_2D_2 . The reaction network in Fig. 5 rationalizes these two detections by showing that the energetically likely routes lead to these two species, while the formation of CHD_3 or CH_3D would proceed through a $+ \text{D}_2$ tunneling reaction, which is unlikely to take place at laboratory timescales. Whether it would take place on interstellar timescales depends on the competition with diffusion and needs an astrochemical model for verification.

A.3. Experiment 2: $\text{C} + \text{H}_2 + \text{D} + \text{D}_2$

In experimental series 2 we confirm the detection of CD_4 , CH_2D_2 , and a tentative detection of CH_4 . However, as can be seen from the reaction network in Fig. 5, both CHD_3 and CH_3D could in principle be formed. We attribute the lack of detecting these species to:

1. the existence of a fully barrierless formation pathway for both CD_4 and CH_2D_2 ,
2. the large bandstrength for CH_4 allowing a detection of small amounts,
3. for CHD_3 and CH_3D there is the requirement of at least one reaction that involves tunneling of the type $\text{CH}_n\text{D}_m + \text{H}_2$ which is in direct competition with a barrierless reaction of the type $\text{CH}_n\text{D}_m + \text{D}$.

B. PEAK POSITIONS AND DETECTIONS

In Table 4 the observed peak positions are listed, along with their molecular assignment based on literature values. The last four columns indicate for which of the experiments a particular peak has been detected, with brackets indicating a weak feature.

We confirm the results published by Qasim et al. (2020) who showed that (deuterated) methane is efficiently formed when carbon atoms react with H (D) on a water surface via experiments 1A and 2A. Furthermore, we detect H_2CO and CO_2 . Formaldehyde is present as a product from the reaction between the carbon atom and water (Hickson et al. 2016) and is the topic of a future study (Molpeceres et al. 2021). The presence of H_2CO further leads to the tentative detection of a CH_3OH feature in experiments 1A and 1D at 1015 cm^{-1} as a result of the hydrogenation of formaldehyde (Watanabe & Kouchi 2002; Fuchs et al. 2009; Qasim et al. 2018). CO_2 is a contaminant that arises from atomic carbon sources of this design (Krasnokutski & Huysen 2014; Qasim et al. 2020). Note also the gas-phase CO_2 bands around 2340 cm^{-1} .

C. POTENTIAL ENERGY SURFACES FOR THE C_{2v} AND C_s SYMMETRIES

Figure 6 shows the potential energy cuts for the reaction $\text{C} + \text{H}_2 \longrightarrow \text{CH}_2$, reaction 5, on both C_{2v} and C_s surfaces. Note that for both C_s surfaces at $R > 1.8\text{ Å}$ we faced convergence issues. These values have been omitted. The position of the $^3\text{CH}_2$ ground state is indicated in each figure.

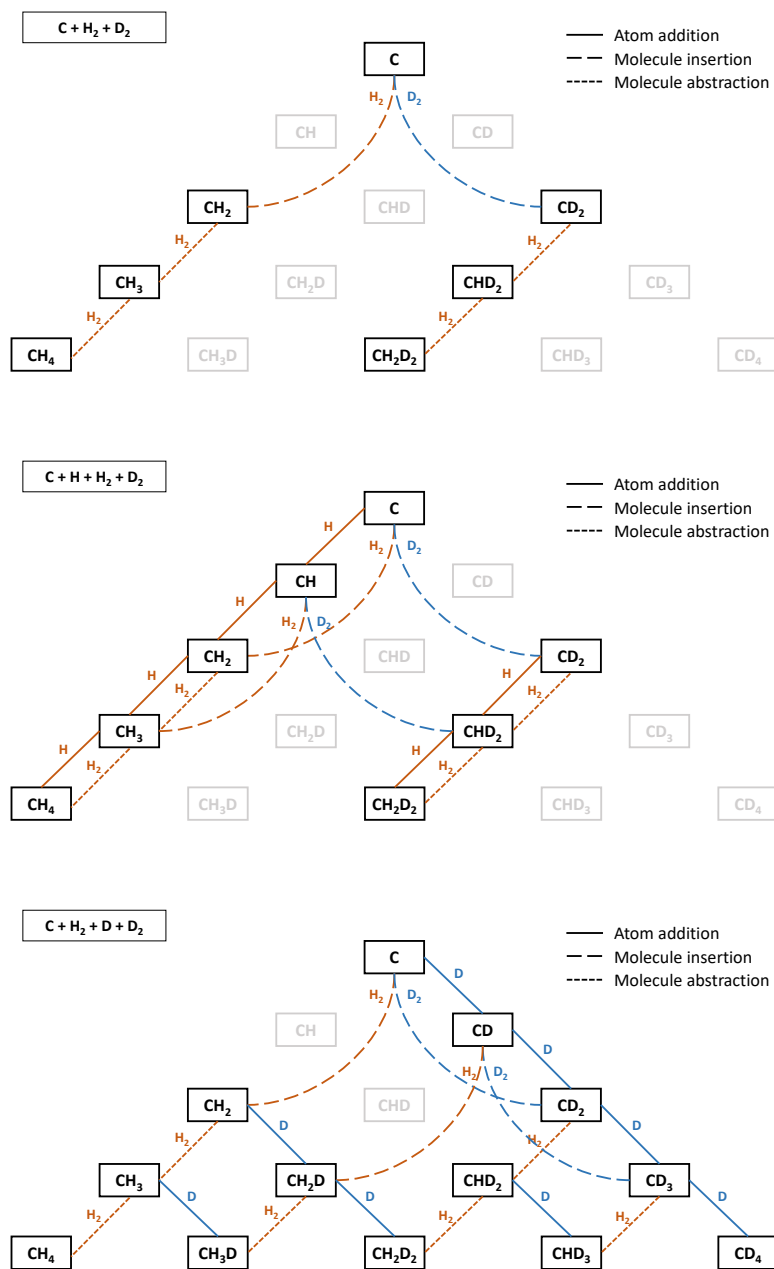


Figure 5. Reaction network for the hydrogenation and deuteration reactions leading to the formation of methane isotopologues. Analogously to Fig. 4, three types of reactions are considered: H or D addition, H₂ or D₂ insertion, and H₂ abstraction.

REFERENCES

- Adler, T. B., Knizia, G., & Werner, H.-J. 2007, JChPh, 127, 221106, doi: [10.1063/1.2817618](https://doi.org/10.1063/1.2817618)
- Albar, J. D., Summerfield, A., Cheng, T. S., et al. 2017, NatSR, 7, 6598, doi: [10.1038/s41598-017-07021-1](https://doi.org/10.1038/s41598-017-07021-1)
- Anton, R., Wiegner, T., Naumann, W., et al. 2000, RSI, 71, 1177, doi: [10.1063/1.1150420](https://doi.org/10.1063/1.1150420)
- Baskin, C. P., Bender, C. F., Bauschlicher, C. W., & Schaefer, H. F. 1974, JChS, 96, 2709, doi: [10.1021/ja00816a008](https://doi.org/10.1021/ja00816a008)
- Bauschlicher, C. W. 1978, CPL, 56, 31, doi: [https://doi.org/10.1016/0009-2614\(78\)80179-1](https://doi.org/10.1016/0009-2614(78)80179-1)
- Bauschlicher, C. W., Haber, K., Schaefer, H. F., & Bender, C. F. 1977, JChS, 99, 3610, doi: [10.1021/ja00453a014](https://doi.org/10.1021/ja00453a014)

Table 4. Summary of all detected peak positions, with the exception of water (H_2O : 3380 and 1660 cm^{-1} and D_2O : 2440 and 1220 cm^{-1}). Experiments in brackets indicate a weak feature or tentative detection

Peak pos. (cm^{-1})	Molecule	Ref.	Detected in Exp. 1	Detected in Exp. 2	Detected in Exp. 3	Detected in Exp. 4
3007	CH_4	[2]	1A, 1B	—	—	(4A)
3000	CH_2D_2	[3]	(1B), 1C	—	—	—
2343	CO_2	[4]	All	All	3A, 3B	^a
2277	CH_2D_2	[3]	1C	(2C)	—	—
2250	CD_4	[5]	—	2A, 2B	—	—
2226	CH_2D_2	[3]	1C	—	—	—
2152	CO	[6]	All	All	3A, 3B	All
2137	CO	[6]	All	All	3A, 3B	All
1717	H_2CO	[7]	All	All	3A, 3B	—
1666	D_2CO	[8]	—	—	—	4A, 4B
1500	H_2CO	[7]	All	All	3A, 3B	—
1430	CH_2D_2	[3]	1B, 1C	—	—	—
1303	CH_4	[1,2]	1A, 1B, (1C)	(2C)	(3B)	4A
1250	H_2CO	[7]	1A	—	3A, 3B	—
1231	CH_2D_2	[3]	1B, (1B)	—	—	—
1102	D_2CO	[8]	—	—	—	(4A), 4B
1083	CH_2D_2	[3]	1B,	(2C)	3B	—
1028	CH_2D_2	[3]	1B, (1B)	(2A), 2B, 2C	3B	—
1015	CH_3OH	[9]	1A, (1B)	—	—	—
993	CD_4	[5]	(1C)	2A, 2B, (2C)	—	—
991	D_2CO	[8]	—	—	—	4A, 4B

References—[1] Shimanouchi (1972) ; [2] Hagen et al. (1983); Quattrocchi & Ewing (1992a); [3] Quattrocchi & Ewing (1992b); [4] Gerakines et al. (1995) ; [5] Chapados & Cabana (1972); Edling et al. (1987); [6] Schmitt et al. (1989); [7] Schutte et al. (1996); [8] Tso & Lee (1984); Nagaoka et al. (2005); [9] Qasim et al. (2018)

^aOverlaps with the D_2O stretch mode

- Becke, A. D. 1988, *PhRvA*, 38, 3098,
doi: [10.1103/PhysRevA.38.3098](https://doi.org/10.1103/PhysRevA.38.3098)
- . 1993, *JChPh*, 98, 5648, doi: [10.1063/1.464913](https://doi.org/10.1063/1.464913)
- Beyer, A. N., Richardson, J. O., Knowles, P. J., Rommel, J., & Althorpe, S. C. 2016, *JPCL*, 7, 4374,
doi: [10.1021/acs.jpcllett.6b02115](https://doi.org/10.1021/acs.jpcllett.6b02115)
- Bisbas, T. G., Schruha, A., & van Dishoeck, E. F. 2019, *MNRAS*, 485, 3097, doi: [10.1093/mnras/stz405](https://doi.org/10.1093/mnras/stz405)
- Boogert, A. A., Gerakines, P. A., & Whittet, D. C. 2015, *ARA&A*, 53, 541, doi: [10.1146/annurev-astro-082214-122348](https://doi.org/10.1146/annurev-astro-082214-122348)
- Boogert, A. C. A., Schutte, W. A., Tielens, A. G. G. M., et al. 1996, *A&A*, 315, L377
- Brown, P. D., & Charnley, S. B. 1991, *MNRAS*, 249, 69,
doi: [10.1093/mnras/249.1.69](https://doi.org/10.1093/mnras/249.1.69)
- Brown, P. D., Charnley, S. B., & Millar, T. J. 1988, *MNRAS*, 231, 409, doi: [10.1093/mnras/231.2.409](https://doi.org/10.1093/mnras/231.2.409)
- Burton, M. G., Ashley, M. C. B., Braiding, C., et al. 2015, *ApJ*, 811, 13, doi: [10.1088/0004-637X/811/1/13](https://doi.org/10.1088/0004-637X/811/1/13)
- Callan, C. G., & Coleman, S. 1977, *PhRvD*, 16, 1762,
doi: [10.1103/PhysRevD.16.1762](https://doi.org/10.1103/PhysRevD.16.1762)
- Chapados, C., & Cabana, A. 1972, *CaJCh*, 50, 3521,
doi: [10.1139/v72-566](https://doi.org/10.1139/v72-566)
- Chuang, K. J., Fedoseev, G., Qasim, D., et al. 2018, *A&A*, 617, A87, doi: [10.1051/0004-6361/201833439](https://doi.org/10.1051/0004-6361/201833439)
- Cuppen, H. M., & Herbst, E. 2007, *ApJ*, 668, 294,
doi: [10.1086/521014](https://doi.org/10.1086/521014)
- D’Hendecourt, L. B., Allamandola, L. J., & Greenberg, J. M. 1985, *A&A*, 152, 130
- Duchovic, R. J., & Hase, W. L. 1985, *JChPh*, 82, 3599,
doi: [10.1063/1.448918](https://doi.org/10.1063/1.448918)
- Duflot, D., Toubin, C., & Monnerville, M. 2021, *FrASS*, 8, 24,
doi: [10.3389/fspas.2021.645243](https://doi.org/10.3389/fspas.2021.645243)
- Dunning, Thom H., J. 1989, *JChPh*, 90, 1007,
doi: [10.1063/1.456153](https://doi.org/10.1063/1.456153)
- Dunning, T. H., Peterson, K. A., & Wilson, A. K. 2001, *JChPh*, 114, 9244, doi: [10.1063/1.1367373](https://doi.org/10.1063/1.1367373)
- Edling, J. A., Richardson, H. H., & Ewing, G. E. 1987, *JMoSt*, 157, 167, doi: [https://doi.org/10.1016/0022-2860\(87\)87091-6](https://doi.org/10.1016/0022-2860(87)87091-6)
- Fredon, A., Groenenboom, G. C., & Cuppen, H. M. 2021, *ESC*, 5, 2032–2041, doi: [10.1021/acsearthspacechem.1c00116](https://doi.org/10.1021/acsearthspacechem.1c00116)

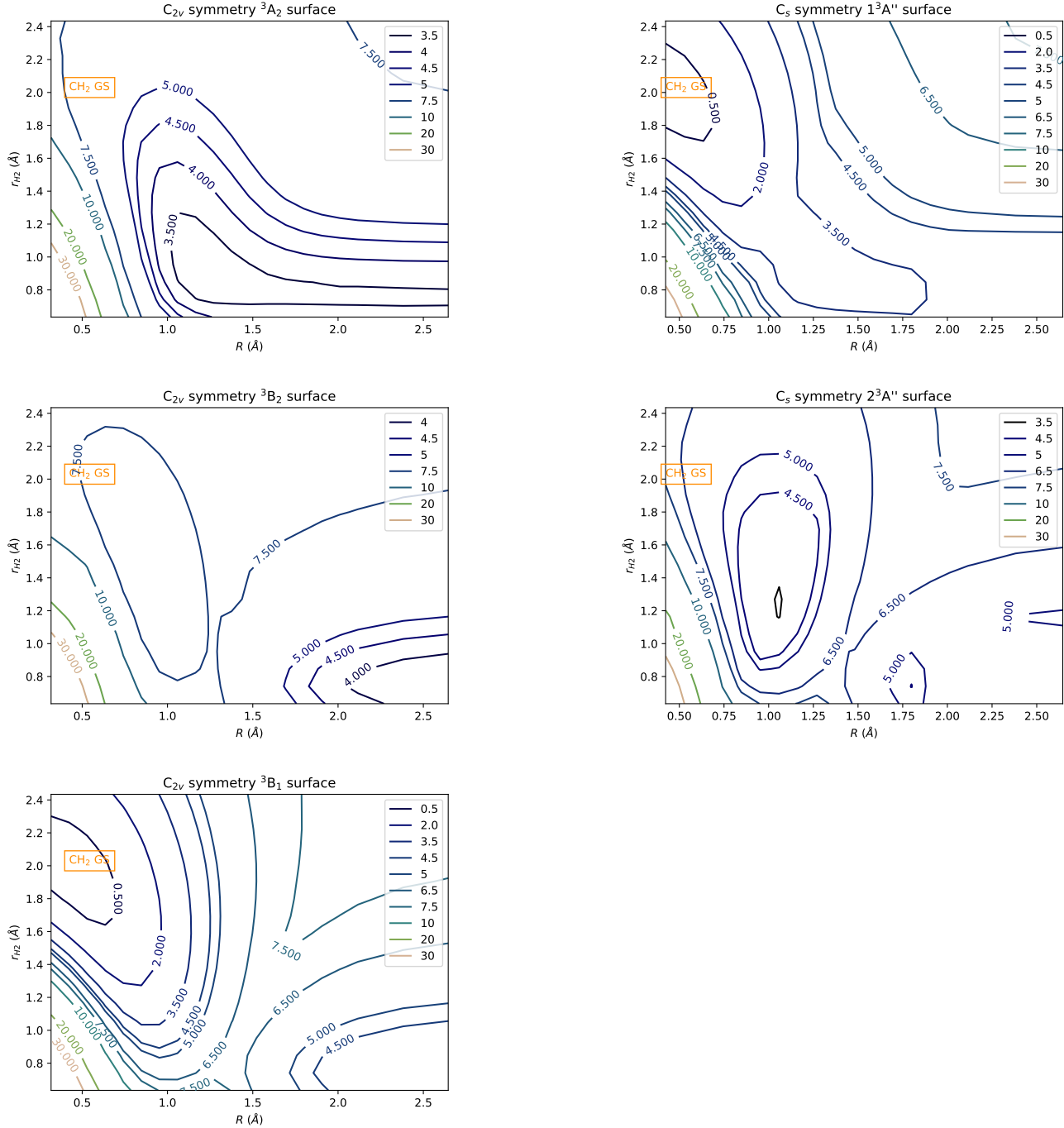


Figure 6. Potential energy cuts for the reaction C + H₂ on three C_{2v} (left column) and two C_s symmetry (right column) surfaces.

Fuchs, G. W., Cuppen, H. M., Ioppolo, S., et al. 2009, A&A, 505, 629, doi: [10.1051/0004-6361/200810784](https://doi.org/10.1051/0004-6361/200810784)
 Furuya, K., Aikawa, Y., Hincelin, U., et al. 2015, A&A, 584, A124, doi: [10.1051/0004-6361/201527050](https://doi.org/10.1051/0004-6361/201527050)
 Gamallo, P., Defazio, P., Akpinar, S., & Petrongolo, C. 2012, JPCA, 116, 8291, doi: [10.1021/jp304125m](https://doi.org/10.1021/jp304125m)
 Garrod, R. T. 2013, ApJ, 778, 158, doi: [10.1088/0004-637X/778/2/158](https://doi.org/10.1088/0004-637X/778/2/158)

Gerakines, P. A., Schutte, W. A., Greenberg, J. M., & van Dishoeck, E. F. 1995, A&A, 296, 810.
<https://arxiv.org/abs/astro-ph/9409076>
 Goldsmith, P. F., & Li, D. 2005, ApJ, 622, 938, doi: [10.1086/428032](https://doi.org/10.1086/428032)
 González, M., Saracibar, A., & Garcia, E. 2011, PCCP, 13, 3421, doi: [10.1039/C0CP01188F](https://doi.org/10.1039/C0CP01188F)
 Greenler, R. G. 1966, JChPh, 44, 310, doi: [10.1063/1.1726462](https://doi.org/10.1063/1.1726462)

- Hagen, W., Tielens, A. G. G. M., & Greenberg, J. M. 1983, *A&AS*, 51, 389
- Harding, L., Guadagnini, R., & Schatz, G. 1993, *JPhCh*, 97, 5472
- Hasegawa, T. I., & Herbst, E. 1993, *MNRAS*, 261, 83, doi: [10.1093/mnras/261.1.83](https://doi.org/10.1093/mnras/261.1.83)
- Henning, T. K., & Krasnokutski, S. A. 2019, *NatAs*, 3, 568, doi: [10.1038/s41550-019-0729-8](https://doi.org/10.1038/s41550-019-0729-8)
- Hickson, K. M., Loison, J.-C., Nuñez-Reyes, D., & Méreau, R. 2016, *JPCL*, 7, 3641, doi: [10.1021/acs.jpcllett.6b01637](https://doi.org/10.1021/acs.jpcllett.6b01637)
- Hiraoka, K., Miyagoshi, T., Takayama, T., Yamamoto, K., & Kihara, Y. 1998, *ApJ*, 498, 710, doi: [10.1086/305572](https://doi.org/10.1086/305572)
- Hunter, J. D. 2007, *CSE*, 9, 90, doi: [10.1109/MCSE.2007.55](https://doi.org/10.1109/MCSE.2007.55)
- Ioppolo, S., Cuppen, H. M., Romanzin, C., van Dishoeck, E. F., & Linnartz, H. 2008, *ApJ*, 686, 1474, doi: [10.1086/591506](https://doi.org/10.1086/591506)
- Ioppolo, S., Fedoseev, G., Lamberts, T., Romanzin, C., & Linnartz, H. 2013, *RSI*, 84, 073112, doi: [10.1063/1.4816135](https://doi.org/10.1063/1.4816135)
- Janssen, C. L., & Nielsen, I. M. 1998, *CPL*, 290, 423, doi: [https://doi.org/10.1016/S0009-2614\(98\)00504-1](https://doi.org/10.1016/S0009-2614(98)00504-1)
- Kästner, J., Carr, J. M., Keal, T. W., et al. 2009, *JPCA*, 113, 11856, doi: [10.1021/jp9028968](https://doi.org/10.1021/jp9028968)
- Keene, J., Blake, G. A., Phillips, T. G., Huggins, P. J., & Beichman, C. A. 1985, *ApJ*, 299, 967, doi: [10.1086/163763](https://doi.org/10.1086/163763)
- Kendall, R. A., Dunning, T. H., & Harrison, R. J. 1992, *JChPh*, 96, 6796, doi: [10.1063/1.462569](https://doi.org/10.1063/1.462569)
- Kim, G.-S., Nguyen, T. L., Mebel, A. M., Lin, S. H., & Nguyen, M. T. 2003, *JPCA*, 107, 1788, doi: [10.1021/jp0261410](https://doi.org/10.1021/jp0261410)
- Kluyver, T., Ragan-Kelley, B., Pérez, F., et al. 2016, in *Positioning and Power in Academic Publishing: Players, Agents and Agendas*, ed. F. Loizides & B. Schmidt (Netherlands: IOS Press), 87–90. <https://eprints.soton.ac.uk/403913/>
- Knizia, G., Adler, T. B., & Werner, H.-J. 2009, *JChPh*, 130, 054104, doi: [10.1063/1.3054300](https://doi.org/10.1063/1.3054300)
- Koning, J., Kroes, G. J., & Arasa, C. 2013, *JChPh*, 138, 104701, doi: [10.1063/1.4793733](https://doi.org/10.1063/1.4793733)
- Krasnokutski, S. A., & Huisken, F. 2014, *ApPhL*, 105, 113506, doi: [10.1063/1.4895806](https://doi.org/10.1063/1.4895806)
- Krasnokutski, S. A., Kuhn, M., Renzler, M., et al. 2016, *ApJ*, 818, L31, doi: [10.3847/2041-8205/818/2/L31](https://doi.org/10.3847/2041-8205/818/2/L31)
- Lacy, J. H., Carr, J. S., Evans, Neal J., I., et al. 1991, *ApJ*, 376, 556, doi: [10.1086/170304](https://doi.org/10.1086/170304)
- Lambert, N., Kaltsoyannis, N., Price, S. D., Žabka, J., & Herman, Z. 2006, *JPCA*, 110, 2898, doi: [10.1021/jp052981d](https://doi.org/10.1021/jp052981d)
- Lamberts, T., Cuppen, H. M., Ioppolo, S., & Linnartz, H. 2013, *PCCP*, 15, 8287, doi: [10.1039/C3CP00106G](https://doi.org/10.1039/C3CP00106G)
- Lamberts, T., Samanta, P. K., Köhn, A., & Kästner, J. 2016, *PCCP*, 18, 33021, doi: [10.1039/C6CP06457D](https://doi.org/10.1039/C6CP06457D)
- Langer, W. 1976, *ApJ*, 206, 699, doi: [10.1086/154430](https://doi.org/10.1086/154430)
- Lee, C., Yang, W., & Parr, R. G. 1988, *PhRvB*, 37, 785, doi: [10.1103/PhysRevB.37.785](https://doi.org/10.1103/PhysRevB.37.785)
- Li, J., Chen, J., Zhao, Z., et al. 2015, *JChPh*, 142, 204302, doi: [10.1063/1.4921412](https://doi.org/10.1063/1.4921412)
- McIlroy, A., & Tully, F. P. 1993, *JChPh*, 99, 3597, doi: [10.1063/1.466156](https://doi.org/10.1063/1.466156)
- Medvedev, D. M., Harding, L. B., & *, S. K. G. 2006, *MolPh*, 104, 73, doi: [10.1080/00268970500238663](https://doi.org/10.1080/00268970500238663)
- Meisner, J., Lamberts, T., & Kästner, J. 2017, *ESC*, 1, 399, doi: [10.1021/acsearthspacechem.7b00052](https://doi.org/10.1021/acsearthspacechem.7b00052)
- Metz, S., Kästner, J., Sokol, A. A., Keal, T. W., & Sherwood, P. 2014, *Wiley Interdiscip. Rev. Comput. Mol. Sci.*, 4, 101, doi: [10.1002/wcms.1163](https://doi.org/10.1002/wcms.1163)
- Miller, K. J. 1975, *JChPh*, 62, 1759, doi: [10.1063/1.430701](https://doi.org/10.1063/1.430701)
- Miyauchi, N., Hidaka, H., Chigai, T., et al. 2008, *CPL*, 456, 27, doi: <https://doi.org/10.1016/j.cplett.2008.02.095>
- Molpeceres, G., Kästner, J., Schömig, R., et al. 2021, *JPCL*, submitted
- Murrell, J. N., Pedley, J. B., & Durmaz, S. 1973, *J. Chem. Soc., Faraday Trans. 2*, 69, 1370, doi: [10.1039/F29736901370](https://doi.org/10.1039/F29736901370)
- Nagaoka, A., Watanabe, N., & Kouchi, A. 2005, *ApJ*, 624, L29, doi: [10.1086/430304](https://doi.org/10.1086/430304)
- Öberg, K. I., Boogert, A. C. A., Pontoppidan, K. M., et al. 2008, *ApJ*, 678, 1032, doi: [10.1086/533432](https://doi.org/10.1086/533432)
- Papadopoulos, P. P., Thi, W. F., & Viti, S. 2004, *MNRAS*, 351, 147, doi: [10.1111/j.1365-2966.2004.07762.x](https://doi.org/10.1111/j.1365-2966.2004.07762.x)
- Peterson, K. A., Adler, T. B., & Werner, H.-J. 2008, *JChPh*, 128, 084102, doi: [10.1063/1.2831537](https://doi.org/10.1063/1.2831537)
- Qasim, D., Chuang, K.-J., Fedoseev, G., et al. 2018, *A&A*, 612, A83, doi: [10.1051/0004-6361/201732355](https://doi.org/10.1051/0004-6361/201732355)
- Qasim, D., Fedoseev, G., Chuang, K. J., et al. 2020, *NatAs*, doi: [10.1038/s41550-020-1054-y](https://doi.org/10.1038/s41550-020-1054-y)
- Qasim, D., Witlox, M. J. A., Fedoseev, G., et al. 2020, *RSciI*, 91, 054501, doi: [10.1063/5.0003692](https://doi.org/10.1063/5.0003692)
- Quattrocci, L. M., & Ewing, G. E. 1992a, *JChPh*, 96, 4205, doi: [10.1063/1.462839](https://doi.org/10.1063/1.462839)
- . 1992b, *CPL*, 197, 308, doi: [https://doi.org/10.1016/0009-2614\(92\)85774-5](https://doi.org/10.1016/0009-2614(92)85774-5)
- Richardson, J. O. 2016, *JChPh*, 144, 114106, doi: [10.1063/1.4943866](https://doi.org/10.1063/1.4943866)
- Rommel, J. B., & Kästner, J. 2011, *JChPh*, 134, 184107, doi: [10.1063/1.3587240](https://doi.org/10.1063/1.3587240)
- Schmidt, A., Offermann, J., & Anton, R. 1996, *TSF*, 281-282, 105, doi: [10.1016/0040-6090\(96\)08586-0](https://doi.org/10.1016/0040-6090(96)08586-0)
- Schmitt, B., Greenberg, J. M., & Grim, R. J. A. 1989, *ApJL*, 340, L33, doi: [10.1086/185432](https://doi.org/10.1086/185432)
- Schutte, W. A., Gerakines, P. A., Geballe, T. R., van Dishoeck, E. F., & Greenberg, J. M. 1996, *A&A*, 309, 633
- Shimanouchi, T. 1972, *National Standard Reference Data Series*, National Bureau of Standards, 39, 1
- Shimonishi, T., Nakatani, N., Furuya, K., & Hama, T. 2018, *ApJ*, 855, 27, doi: [10.3847/1538-4357/aaa6a](https://doi.org/10.3847/1538-4357/aaa6a)

- Simončič, M., Semenov, D., Krasnokutski, S., Henning, T., & Jäger, C. 2020, *A&A*, 637, A72, doi: [10.1051/0004-6361/202037648](https://doi.org/10.1051/0004-6361/202037648)
- Snow, T. P., & McCall, B. J. 2006, *ARA&A*, 44, 367, doi: [10.1146/annurev.astro.43.072103.150624](https://doi.org/10.1146/annurev.astro.43.072103.150624)
- Tso, T. L., & Lee, E. K. C. 1984, *JPhCh*, 88, 5475, doi: [10.1021/j150667a006](https://doi.org/10.1021/j150667a006)
- van de Hulst, H. C. 1946, *RAOU*, 11
- . 1949, The solid particles in interstellar space.
- van der Walt, S., Colbert, S. C., & Varoquaux, G. 2011, *CSE*, 13, 22, doi: [10.1109/MCSE.2011.37](https://doi.org/10.1109/MCSE.2011.37)
- van Dishoeck, E. F., & Black, J. H. 1988, *ApJ*, 334, 771, doi: [10.1086/166877](https://doi.org/10.1086/166877)
- van Harrevelt, R., van Hemert, M. C., & Schatz, G. C. 2002, *JChPh*, 116, 6002, doi: [10.1063/1.1459416](https://doi.org/10.1063/1.1459416)
- Vasyunin, A. I., & Herbst, E. 2013, *ApJ*, 762, 86, doi: [10.1088/0004-637X/762/2/86](https://doi.org/10.1088/0004-637X/762/2/86)
- Wakelam, V., Loison, J. C., Mereau, R., & Ruaud, M. 2017, *MolAs*, 6, 22, doi: [10.1016/j.molap.2017.01.002](https://doi.org/10.1016/j.molap.2017.01.002)
- Wakelam, V., Loison, J. C., Herbst, E., et al. 2015, *ApJS*, 217, 20, doi: [10.1088/0067-0049/217/2/20](https://doi.org/10.1088/0067-0049/217/2/20)
- Watanabe, N., & Kouchi, A. 2002, *ApJL*, 571, L173, doi: [10.1086/341412](https://doi.org/10.1086/341412)
- Werner, H., & Knowles, P. J. 1988, *JChPh*, 89, 5803, doi: [10.1063/1.455556](https://doi.org/10.1063/1.455556)
- Werner, H.-J., Knowles, P. J., Knizia, G., Manby, F. R., & Schütz, M. 2012, *WIREs Comput Mol Sci*, 2, 242
- Werner, H.-J., Knowles, P. J., Knizia, G., et al. 2018, *MOLPRO*, version 2018.1, a package of ab initio programs
- Werner, H.-J., Knowles, P. J., Manby, F. R., et al. 2020, *JChPh*, 152, 144107, doi: [10.1063/5.0005081](https://doi.org/10.1063/5.0005081)
- Woon, D. E., & Dunning, T. H. 1993, *JChPh*, 98, 1358, doi: [10.1063/1.464303](https://doi.org/10.1063/1.464303)